Whole Genome Sequencing Highlights the Pathogenic Profile in *Nocardia* Keratitis

Xiaoyan Guo, Zijun Zhang, Qiankun Chen, Leying Wang, Xizhan Xu, Zhenyu Wei, Yang Zhang, Kexin Chen, Zhiqun Wang, Xinxin Lu, and Qingfeng Liang

Beijing Institute of Ophthalmology, Beijing Tongren Eye Center, Beijing Tongren Hospital, Capital Medical University, Beijing, China

Correspondence: Qingfeng Liang, Beijing Institute of Ophthalmology, Beijing Tongren Eye Center, Beijing Tongren Hospital, Capital Medical University, Beijing 100005, China; lqflucky@163.com.

Received: August 26, 2023
Accepted: February 26, 2024
Published: March 19, 2024

Citation: Guo X, Zhang Z, Chen Q, et al. Whole genome sequencing highlights the pathogenic profile in *Nocardia* keratitis. *Invest Ophthalmol Vis Sci.* 2024;65(3):26. https://doi.org/10.1167/iovs.65.3.26

Purpose. *Nocardia* keratitis is a serious and sight-threatening condition. This study aims to reveal the virulence and antimicrobial resistance gene profile of *Nocardia* strains using whole genome sequencing.

Methods. Whole-genome sequencing was performed on 23 cornea-derived *Nocardia* strains. Together with genomic data from the respiratory tract and the environment, 141 genomes were then utilized for phylogenetic and pan-genome analyses, followed by virulence and antibiotic resistance analysis. The correlations between virulence genes and pathogenicity were experimentally validated, including the characteristics of *Nocardia* colonies and clinical and histopathological evaluations of *Nocardia* keratitis mice models.

Results. Whole-genome sequencing of 141 *Nocardia* strains revealed a mean of 220 virulence genes contributed to bacterial pathogenesis. The *mce* gene family analysis led to the categorization of strains from the cornea into groups A, B, and C. The colonies of group C had the largest diameter, height, and fastest growth rate. The size of corneal ulcers and the clinical scores showed a significant increase in mouse models induced by group C. The relative expression levels of pro-inflammatory cytokines (CD4, IFN-γ, IL-6Rα, and TNF-α) in the lesion area exhibited an increasing trend from group A to group C. Antibiotic resistance genes (ARGs) spanned nine distinct drug classes, four resistance mechanisms, and seven primary antimicrobial resistance gene families.

Conclusions. Whole genome sequencing highlights the pathogenic role of *mce* gene family in *Nocardia* keratitis. Its distribution pattern may contribute to the distinct characteristics of the growth of *Nocardia* colonies and the clinical severity of the mice models.

Keywords: *Nocardia* keratitis, whole genome sequencing, *mce* gene family, colony growth pattern, animal model

Nocardia, a genus classified within the family *Nocardiaceae*, under the order *Mycobacteriales* within the class *Actinomycetes*,[1] is commonly found in soil, dust, and decaying organic material.[2] *Nocardia* can infect various organs in the human body, with the lungs, skin, and cornea being the most common sites.[3] To date, more than 100 *Nocardia* species have been identified through 16S rRNA gene sequencing analysis, and 9 common species or complexes are closely associated with human diseases.[4] As the cornea is exposed to environmental stress, *Nocardia* keratitis often arises after corneal trauma or surgery.[5]

Nocardia strains are obligate aerobes with limited nutritional requirements, exhibiting resistance to destruction by neutrophils and macrophages.[6] Moreover, *Nocardia* has the capability to survive and replicate slowly within inflammatory cells, leading to the frequent development of refractory infections with prolonged course.[4] *Nocardia* keratitis, as a severe and sight-threatening condition, presents as a chronic, persistent infection that is unresponsive to commonly used antibiotics.[5] In clinical settings, the manifestations of *Nocardia* keratitis are notably variable, sharing close similarities with fungal and other bacterial keratitis. Consequently, this similarity poses intricate challenges for timely and precise early-stage differential diagnosis.[7] Additionally, consistent variations in the severity of *Nocardia* keratitis were observed among patients with similar presentation times, along with diverse clinical manifestations and outcomes among patients infected with the same *Nocardia* species, as identified through mass spectrometry and sequencing analysis.[8,9] These observations revealed the difficulties in determining the severity and prognosis of *Nocardia* keratitis based on the species of the strains, which emphasized the need for further investigation into the clinical features and pathogenesis underlying *Nocardia* keratitis.

Whole genome sequencing (WGS), as a high-throughput sequencing technology, has significantly promoted clinical microbial research at the gene level and generated diverse applications.[10] Studies have exhibited that WGS can be exploited to detect the comprehensive presence of virulence genes and antimicrobial resistance (AMR) genes

iovs.arvojournals.org | ISSN: 1552-5783

among clinical bacterial strains.[10,11] Thus, by analyzing the pathogenicity, antimicrobial susceptibility, the ability to form biofilms, and survival in various environments of bacteria, the bacterial genetic profiles and functional phenotypes can be predicted, thereby guiding appropriate clinical diagnosis and treatment strategies.

In this study, we aim to integrate clinical features and conduct a comprehensive genomic analysis to identify the pathogenic traits of *Nocardia* in a clinical cohort of 23 patients. Additionally, we seek to identify virulence genes that correlate with the severity of clinical lesions. This integrated approach will support the development of a more precise and tailored diagnostic classification for *Nocardia* keratitis.

Materials and Methods

Establishment of *Nocardia* Keratitis Cohort

Twenty-three consecutive patients (23 eyes) with *Nocardia* keratitis were included in the study, from the Department of Ophthalmology at Beijing Tongren Hospital, Capital Medical University between 2003 and 2022. The inclusion criteria were patients with typical clinical manifestations of *Nocardia* keratitis and at least one positive etiological examination (corneal scraping and microbial culture). Informed consent was signed after explicating the study purposes and examination content to the patients. Basic information (age, sex, and first visit time), complete medical history (risk factor and presentation time), and clinical and etiological examination results (visual acuity before treatment, clinical manifestation, corneal scraping, culture, in vivo confocal microscopy, visual acuity after treatment, and resolution time) were collected. Based on the infectious corneal ulcer scoring system,[12] the severity of patients with *Nocardia* keratitis was evaluated as mild, moderate, and severe. This study adhered to the tenets of the Declaration of Helsinki and obtained the approval of Beijing Tongren Hospital, Capital Medical University Ethics Committee (TRECKY2021-024).

Identification and Antimicrobial Susceptibility Testing of *Nocardia* Strains From the Cornea

A total of 23 strains of *Nocardia* were isolated from corneal scrapings between 2003 and 2022 and stored at −80°C in the Ocular Microbial Resource Bank (OMRB) at the Beijing Institute of Ophthalmology, China. To revive the strains, they were inoculated on blood agar plates (BAPs; Thermo Fisher Scientific, Waltham, MA, USA) and cultured in a bacterial incubator (Thermo Fisher Scientific, Waltham, MA, USA) at 35°C for 3 days. After purification using the streak plate method, the strains were identified to the species level using matrix-assisted laser desorption/ionization-time of flight mass spectrometry (Smart MS; DL Biotech, Zhuhai, China).

To perform the antimicrobial susceptibility testing, 23 strains of freshly grown *Nocardia* isolated from the cornea were added to deionized water and adjusted to 0.5 McFarland using a turbidimeter (Thermo Fisher Scientific, Waltham, MA, USA).[13–15] Next, 100 µL of the suspension was transferred into 11 mL of Mueller Hinton broth medium (Thermo Fisher Scientific, Waltham, MA, USA). After mixing the suspension to no visible precipitate, 100 µL of the mixture was introduced into every well of a 96-well plate, which was then combined with lyophilized antibiotics (ceftriaxone, clarithromycin, imipenem, linezolid, rifampin, tobramycin, vancomycin, moxifloxacin, amikacin, and trimethoprim-sulfamethaxole) in each respective well (Thermo Fisher Scientific, Waltham, MA, USA). The plates were sealed and incubated at 35°C for 24 to 72 hours. Final results were based on the 72-hour data, following cutoffs specified in the Clinical and Laboratory Standards Institute (CLSI) M62 document.

Whole Genome Sequencing and Annotation of Cornea-Derived *Nocardia* Strains

Subsequently, genomic DNA (gDNA) was extracted from each strain using the DNA isolation mini kit-box2 (DC103-01; Vazyme, Nanjing, China). The concentration and purity of the gDNA samples were evaluated using Nanodrop2000 (Thermo Fisher Scientific, Waltham, MA, USA). The gDNA samples were then submitted for whole genome sequencing on the Illumina Novaseq platform in the PE150 mode (Novogene, Tianjin, China), ensuring that all sequencing depths exceeded 100 folds. The raw data obtained from the WGS were filtered to remove low-quality data, including reads containing low-quality bases (>40%), reads containing >10% N, and reads with an overlap between adapters exceeding 15 bp. This filtering process was performed using readfq 10 (https://github.com/cjfields/readfq). The remaining clean data were de novo assembled by SPAdes 3.15.5,[16] and the coding sequences (CDSs) were predicted using Prokka 1.14.5.[17]

Phylogenetic Analysis and Pan-Genome Analysis

To gain a more comprehensive understanding of the biological functions and pathogenicity of *Nocardia* strains isolated from corneal lesions, it is crucial to conduct a thorough analysis of the phylogenetic relationship and virulence genes from various sources of *Nocardia*. As a result, we downloaded the whole genome sequences of 81 *Nocardia* strains isolated from the respiratory tract and 41 *Nocardia* strains isolated from the environment from the National Center for Biotechnology Information (https://www.ncbi.nlm.nih.gov/datasets/genome/). The quality control of 145 genome assemblies was carried out using QUAST 5.2 (CAB, St. Petersburg, Russia).[18] The inclusion criteria were N_{75} value > 10,000 bp, undetermined bases < 500 per 100,000 bases, and completeness > 98%. As a result, 141 *Nocardia* genomes that met the quality control standards were identified at the species (132 strains) or genus (9 strains) level and subjected to phylogenetic analysis using GTDB-Tk 2.3.2.[19] The phylogenetic tree was visualized using iTOL 6.8 (https://itol.embl.de/).[20] Pan-genome analysis, including core genome, accessory genome, and unique genome, was performed using Bactopia 2.2.0[21] and Bacterial Pan-Genome Analysis 4.6.6 (BPGA).[22] Furthermore, based on clusters of orthologous groups (COGs),[23] the functional genes were categorized into 20 categories (from category C to category V).

Analysis of Virulence Genes and Antibiotic Resistance Genes

The protein sequences of 141 genomes were aligned using BLASTp version 2.13.0 with specific criteria: a cutoff of 40% identity, 70% coverage, and an E value of 1e-10 against the Virulence Factor Database (VFDB).[24] The adherence, inva-

Investigative Ophthalmology & Visual Science

sion, and other virulence genes were identified. Based on the specific distribution and presence of certain virulence genes, the 23 strains of *Nocardia* isolated from the cornea were grouped into 3 clusters (group A, group B, and group C) using R software version 4.2.2 (The R Foundation, Vienna, Austria). This clustering analysis will help us identify and validate the distinct virulence genes, which in turn will aid in assessing the severity and prognosis of *Nocardia* keratitis. At last, the antibiotic resistance genes (ARGs) were identified using Resistance Gene Identifier (RGI) version 6.0.2 with a cutoff of 60% identity and 70% coverage against the Comprehensive Antibiotic Resistance Database (CARD).[25]

Experimental Validation of Virulence Genes as Criteria for Grouping Corneal Pathogenicity

Characteristics Analysis of *Nocardia* Colonies. Three strains from each group (group A, group B, and group C) of *Nocardia* were cultured on BAPs and incubated at 35°C for 3 days. The growth of *Nocardia* colonies was observed and photographed every 12 hours using a slit lamp microscope (Topcon SL-D7, Tokyo, Japan). At the same time, the cross-sections of the colonies were captured using a telecentric optical coherence tomography (OCT) cornea lens by Optovue iVue 80 (Fremont, CA, USA). The diameter, height, and angle (elevation angle) of the colonies were measured using the software in Optovue iVue 80, and each parameter was calculated as the mean value of 3 colonies.

Establishment of a Mouse Model of *Nocardia* Keratitis. Twelve 8-week-old female C57BL/6N mice were purchased from Vital River Laboratory Animal Technology Co., Ltd. (Beijing, China) and kept in a specific pathogen-free animal room for 1 week. They were then divided into four groups with the random number table: a control group (corneal stroma injection with 2 µL phosphate-buffered solution) and three *Nocardia* keratitis groups (group A, group B, and group C). Only the left eyes of each mouse were used for the experiments. The right eyes of each mouse model were set as absolute control and were intact throughout the animal experiments. Three strains from each group of freshly grown *Nocardia* were diluted with Mueller Hinton broth medium (Thermo Fisher Scientific, Waltham, MA, USA). The selected dosage for the corneal stroma injection was 2 µL of the diluent at a concentration of 1.5×10^8 colony forming unit (CFU)/mL, based on the bacterial keratitis mouse model by Chojnacki et al.[26] and our preliminary experiments.[27–29] Corneal scrapings of the mice were performed 1 day after the injection, and positive for weak acid-fast staining indicated the mouse model was established successfully. All animal studies followed the guidelines of the Association for Research in Vision and Ophthalmology and were approved by the Institutional Animal Care and Use Committee.

Clinical and Histopathological Evaluations of the Models. The models with *Nocardia* keratitis were examined daily to monitor the disease progression and photographed with a slit lamp microscope (Topcon SL-D7, Tokyo, Japan) on day 1, day 3, and day 7. Additionally, 1 mL of 1% sodium fluorescein was instilled into the inferior conjunctival sac of the mice, and the corneal staining patterns were photographed and fitted with a cobalt blue filter. The diameter of the corneal ulcer was measured manually with the photographs of sodium fluorescein staining, and the clinical scores (ranging from 0 to 4) were determined based on the observable severity of ocular disease in the infected mice.[30] The mice were euthanized on day 7, and their cornea tissues were preserved in 4% paraformaldehyde solution and conducted hematoxylin and eosin (H&E) staining for histological analysis under a light microscope (Olympus BX51; Olympus, Tokyo, Japan).

Colony Forming Unit Assessment of the Models. The left corneas were enucleated and homogenized into 1.0 mL sterile phosphate-buffered solution (PBS) using tissue grinder (Kimble Kontes Dounce, Rockwood, TN, USA) on day 1, day 3, and day 7 post-infection. To assess the CFU of *Nocardia* isolated from the models, 0.1 mL of the homogenate was serially diluted 1:10 in PBS. Serial dilutions (0.1 mL/plate) were plated onto BAP (Thermo Fisher Scientific, Waltham, MA, USA) in triplicate and incubated at 35 °C for 3 days. After the colonies were counted, CFU/mL were calculated.

Immunohistochemistry and Immunofluorescence Staining. For CD4 and IFN-γ staining, slides with 5-µm-thick sections were deparaffinized in xylene and rehydrated using a series of alcohol concentrations (from 100% to 70%). Antigen retrieval for CD4 and IFN-γ staining was performed in a microwave oven using specific buffer solutions. Endogenous peroxidase activity was blocked using 3% hydrogen peroxide for 10 minutes. The samples were then blocked with 5% goat serum in PBS for 1 hour. Primary antibodies (CD4 and IFN-γ, 1:1000; Abcam, Cambridge, UK) were applied to the slides and left to incubate overnight at 4°C. After washing with PBS, the slides were treated with HRP-conjugated goat anti-rabbit IgG (1:1000; Abcam, Cambridge, UK) for 1 hour at room temperature. Subsequently, the slides were visualized using the 3, 3-diaminobenzidine (DAB; Beyotime Biotech, Guangzhou, China) kit and counterstained with hematoxylin. Finally, the stained sections were observed under a light microscope at 400-fold magnification (Olympus BX51; Olympus, Tokyo, Japan), and three fields of view per section were selected for further analysis. For immunofluorescence staining of IL-6Rα and TNF-α, following the above procedures, the slides were incubated at 4°C overnight with the primary antibodies (IL-6Rα: 1:200; Santa Cruz, Dallas, TX, USA; and TNF-α: 1:100; Abcam, Cambridge, UK). After washing with PBS, slides were incubated with Alexa Fluor 488-conjugated goat anti-mouse IgG (1:500; Abcam, Cambridge, UK) for 1 hour in a dark room. Cell nuclei were counterstained with 4, 6-diamidino-2-phenylindole dihydrochloride (DAPI; Sigma-Aldrich, Darmstadt, Germany). Slides were washed and examined using a fluorescent microscope (Olympus DP72, Tokyo, Japan) with 400-fold magnification.

Statistical Analysis

All bioinformatics data were analyzed and visualized using R software 4.2.2 (The R Foundation, Vienna, Austria). Wilcoxon rank-sum tests were used to compare corneal genomes with respiratory or environmental genomes within core, accessory, and unique genomes. Parameters such as *Nocardia* colony size, clinical scores of mice models with *Nocardia* keratitis, CFU of *Nocardia*, and staining results were analyzed using GraphPad Prism 9.0 software (GraphPad, La Jolla, CA, USA). Statistical significance was determined using 1-way analysis of variance (ANOVA) followed by the Tukey post hoc test. All P values were 2-tailed, and $P < 0.05$ was considered statistically significant.

Investigative Ophthalmology & Visual Science

Results

Nocardia Keratitis Cohort

In this study, a total of 23 patients (23 eyes) diagnosed with *Nocardia* keratitis were included, and their average age was 40.34 ± 3.49 years. All of them had unilateral infections, and 16 of them (69.6%) were men. Among these patients, seven cases had a history of trauma (3 cases caused by vegetable materials), six cases had a history of contact lens wear, and two had a history of surgery (keratoplasty and meningioma surgery). The mean duration from symptoms onset to hospital admission was 20.50 ± 2.86 days. Based on the clinical manifestations, patients were categorized into three severity levels: mild (8 of 23), moderate (6 of 23), and severe (9 of 23). The mean resolution time was 33.00 ± 7.07 days. After medical treatment, 18 patients showed improvement in clinical manifestations and visual acuity. However, 5 out of 23 (all categorized as severe) required procedures, such as penetrating keratoplasty (PKP) or deep anterior lamellar keratoplasty (DALK; Table 1).

Among the *Nocardia* strains isolated from the cornea and identified at the species level, *N. puris were* the most numerous (7 strains, 30.4 %), followed by *N. farcinica* (5 strains, 21.7 %), and *N. abscessus* (4 strains, 17.4 %). To confirm the antimicrobial susceptibility of *Nocardia* isolated from the cornea, the minimum inhibitory concentration (MIC) was examined using the broth microdilution method by CLSI M62, calculated MIC_{50} and MIC_{90}, and finally listed with different species in Table 2. All 23 strains were sensitive to amikacin, imipenem, and linezolid, whereas 13 strains were resistant to rifampin, and 12 strains were resistant to vancomycin. Interestingly, the values of MIC_{50} and MIC_{90} of 2 powerful antibiotics, vancomycin (MIC_{50} = 16 mg × L^{-1} and MIC_{90} = 64 mg × L^{-1}) and rifampin (MIC_{50} = 4 mg × L^{-1} and MIC_{90} = 8 mg × L^{-1}), were notably higher than that of the others. Similarly, except for *N. puris*, over half of the strains in each species were resistant to vancomycin. For the other five antibiotics (ceftriaxone, clarithromycin, tobramycin, trimethoprim-sulfamethaxole, and moxifloxacin), one to eight strains exhibited resistance.

Genomic Characteristics and Whole-Genome Phylogenetic Analysis

After passing quality control filters, the whole genomes of 141 multiple *Nocardia* strains were successfully investigated. The average nucleotide identity (ANI) values for 141 *Nocardia* strains surpassed 95%, underscoring the accuracy of our identification against reference sequences. The mean genome sizes of corneal, respiratory, and environmental genomes were 6.95 Mb, 6.44 Mb, and 6.67 Mb, with mean GC content values of 69.1%, 68.5%, and 66.9%, respectively.

Among the *Nocardia* identified at the species level, *N. farcinica* was the most numerous (34 strains, 24.1%), followed by *N. cyriacigeorgica* (28 strains, 19.9%), *N. puris* (9 strains, 6.4%), and *N. abscessus* (8 strains, 5.7%). To further evaluate the relationship between the strains, a circular whole-genome phylogenetic tree was constructed using the whole genome sequence of 141 multiple *Nocardia* strains (Fig. 1). The label of each strain in the phylogenetic tree consists of the identification results of *Nocardia* and the strain name. Remarkably, most of the same species of *Nocardia* were harbored in the same clade suggesting the accuracy and precision of our whole-genome phylogenetic analysis. The general background profiles including isolated source, collection year, and geographic origin, of 141 multiple *Nocardia* strains were added around the circular whole-genome phylogenetic tree with 3 rings, respectively. The isolated sources from which most strains were obtained were the respiratory tract (79 strains, 56.0%), environment (39 strains, 27.7%), and cornea (23 strains, 16.3%). *Nocardia* isolated from the cornea included seven different species, most of which were *N. puris* (7 of 23). As to the collection year and geographic origin, 65.3% of *Nocardia* were collected in the second decade of the 21st century and China contributed 72.3% (102 strains) of the *Nocardia* whole genome sequence, followed by Venezuela (8 strains, 5.7%), and the United States (5 strains, 3.6%).

Functional Differences of Three Isolated Sources With Pan-Genome Analysis

To further investigate the functional differences among 3 isolated sources, pan-genome analysis was performed among the 141 genomes by BPGA with 50% sequence identity cutoff by default. The corneal genome size comprised 31,959 genes, whereas the number of respiratory and environmental genomes was 45,835 and 60,187 genes. Four hundred twenty-one genes were identified as core genes, shared among all corneal strains, whereas 1458 core genes were present in respiratory duct strains, and 224 core genes in environmental strains. Consequently, the accessory genes numbered 31,538 genes, 44,377 genes, and 59,963 genes for corneal, respiratory, and environmental genomes, respectively (Fig. 2A). Moreover, the corneal, respiratory, and environmental genomes were open, with the Bpan of these genomes less than 1 (0.46, 0.35, and 0.47). Based on the openness of the genomes, the gene function profiles, and the functional differences were further assessed among three isolated sources. The COG categories and annotations of predicted genes within the core, accessory, and unique genomes were evaluated and graphed as stacked bar charts (Fig. 2B). Twenty functional COG categories in 3 isolated sources were observed with significant differences in 2 categories (J and R) of the core genome, 5 categories (H, K, M, P, and Q) of the accessory genome, and 10 categories (E, F, G, H, I, J, K, P, Q, and S) of the unique genome. These data indicated the characteristic living patterns of *Nocardia* from the different sources which were assigned to nucleotide transport and metabolism (category F), cell wall/membrane/envelope biogenesis (category M), and secondary metabolites biosynthesis, transport and catabolism (category Q). Additionally, there is the possibility that other categories hold associations with Nocardial virulence, potentially playing a pivotal role in the onset and progression of *Nocardia* keratitis.

Analysis of Virulence Genes and the *mce* Gene Family

Virulence factors play a crucial role in regulating the initiation and progression of *Nocardia* infection. Based on the virulence genes within the whole genomes of 141 multiple *Nocardia* strains, a dot chart was generated (Fig. 3), and 541 virulence genes were identified using BLASTp against the VFDB database. Each genome had a mean of 220 virulence genes, which contributed to various aspects of bacterial pathogenesis, such as adherence (31 genes on aver-

Investigative Ophthalmology & Visual Science

Table 1. Clinical and Genomic Profiles of 23 Patients With *Nocardia* Keratitis

Patient Number	Age (Years)	Sex	Eye	Collection Year	Risk Factor	Presentation Time (Days)	Visual Acuity Before Treatment	Severity	Corneal Scraping	Culture	IVCM	Visual Acuity After Treatment	Resolution Time (Days)	Strain	Species	GC Content (%)	Genome Size (Mb)
1	9	Female	OS	2003	Trauma	16	CF	Severe	+	+	NA	–	DALK	BIO164	*N. cyriacigeorgica*	69.27	8.32
2	14	Male	OD	2003	Contact lens wear	25	20/200	Moderate	–	+	NA	20/67	12	BIO232	*N. cyriacigeorgica*	68.37	6.22
3	58	Male	OS	2004	Trauma	21	20/400	Moderate	+	+	NA	20/40	13	BIO369	*N. farcinica*	67.58	7.17
4	50	Female	OD	2004	NA	20	CF	Severe	+	+	NA	20/100	16	BIO465	*N. puris*	68.17	6.40
5	46	Male	OS	2005	Trauma	6	20/67	Mild	+	+	NA	20/22	14	BIO633	*N. asiatica*	69.98	6.44
6	54	Male	OS	2005	NA	NA	10/100	Moderate	+	+	NA	20/67	NA	BIO530	*N. farcinica*	68.55	8.02
7	45	Male	OD	2006	NA	NA	20/100	Mild	–	+	NA	20/40	NA	BIO650	*N. wallacei*	70.21	6.52
8	61	Male	OD	2007	NA	NA	10/100	Moderate	–	+	NA	20/50	NA	BIO1034	*N. abscessus*	68.51	7.44
9	56	Male	OD	2012	NA	21	20/200	Mild	–	+	–	20/100	13	BIO2454	*N. abscessus*	69.95	6.09
10	47	Male	OS	2013	Trauma (vegetable material)	28	LP	Severe	+	+	–	–	PKP	BIO2905	*N. puris*	70.21	6.55
11	17	Male	OS	2014	Contact lens wear	30	20/22	Mild	–	+	–	20/20	45	BIO3291	*N. wallacei*	70.35	7.01
12	67	Male	OS	2014	NA	8	20/100	Mild	+	+	–	20/40	20	BIO3406	*N. abscessus*	68.74	7.66
13	26	Male	OD	2015	Trauma (vegetable material)	21	HM	Severe	+	+	+	–	DALK	BIO3975	*N. puris*	66.89	8.20
14	45	Female	OS	2015	NA	60	20/100	Moderate	+	+	+	20/40	25	BIO4145	*N. asteroides*	68.59	6.07
15	43	Female	OD	2017	Contact lens wear	22	20/400	Severe	+	+	+	20/200	90	BIO4762	*N. puris*	69.76	6.72
16	44	Male	OD	2017	Meningioma surgery	9	10/100	Severe	+	+	+	20/40	60	BIO4775	*N. puris*	69.83	6.27
17	40	Female	OS	2018	NA	10	20/100	Mild	+	+	–	20/50	20	BIO5183	*N. asiatica*	70.03	5.94
18	51	Male	OD	2020	Keratoplasty	21	HM	Severe	+	+	+	–	PKP	BIO5594	*N. puris*	68.21	7.32
19	18	Male	OD	2020	Contact lens wear	15	20/67	Moderate	–	+	+	20/40	21	BIO5645	*N. farcinica*	69.28	6.23
20	15	Male	OD	2020	Contact lens wear	34	20/40	Mild	–	+	–	20/25	34	BIO5648	*N. abscessus*	69.89	7.41
21	49	Male	OS	2021	Trauma (vegetable material)	5	20/40	Mild	–	+	+	20/22	18	BIO5761	*N. farcinica*	68.45	6.39
22	48	Female	OS	2022	Trauma	7	CF	Severe	+	+	+	20/100	94	BIO5981	*N. puris*	67.53	8.22
23	25	Female	OD	2022	Contact lens wear	31	HM	Severe	+	+	+	–	DALK	BIO6040	*N. farcinica*	69.68	7.34

Note: CF, counting fingers; DALK, deep anterior lamellar keratoplasty; HM, hand motion; IVCM, in vivo confocal microscopy; LP, light perception; NA, not available; PKP, penetrating keratoplasty.

Table 2. Antimicrobial Susceptibility and MICs of 23 *Nocardia* Isolated From the Cornea ($n = 3$)

Antimicrobial Agents	Breakpoints ($mg \cdot L^{-1}$)	Different Species (n, %)							
		Total (23, 100)	*N. puris* (7, 30.4)	*N. farcinica* (5, 21.7)	*N. abscessus* (4, 17.4)	*N. Wallacei* (2, 8.7)	*N. Asiatica* (2, 8.7)	*N. Cyriacigeorgica* (2, 8.7)	*N. Asteroides* (1, 4.4)
Amikacin	S≤8, R≥16								
MIC_{50} ($mg \cdot L^{-1}$)		0.5	0.5	0.5	0.25	0.25	0.125	0.125	1
MIC_{90} ($mg \cdot L^{-1}$)		2	1	2	0.5	4	0.5	0.25	1
Resistance, *n* (%)		0 (0)	0 (0)	0 (0)	0 (0)	0 (0)	0 (0)	0 (0)	0 (0)
Ceftriaxone	S≤8, 16≤I≤32								
MIC_{50} ($mg \cdot L^{-1}$)		1	1	1	1	0.25	1	0.5	8
MIC_{90} ($mg \cdot L^{-1}$)		4	1	64	4	4	2	1	8
Resistance, *n* (%)		1 (4.3)	0 (0)	1 (20.0)	0 (0)	0 (0)	0 (0)	0 (0)	0 (0)
Clarithromycin	S≤2, I=4, R≥8								
MIC_{50} ($mg \cdot L^{-1}$)		1	4	1	0.5	16	0.25	1	1
MIC_{90} ($mg \cdot L^{-1}$)		16	16	16	32	16	2	1	1
Resistance, *n* (%)		8 (34.8)	3 (42.9)	1 (20.0)	2 (50.0)	2 (100.0)	0 (0)	0 (0)	0 (0)
Imipenem	S≤4, I=8, R≥16								
MIC_{50} ($mg \cdot L^{-1}$)		0.25	0.25	0.5	0.25	0.125	0.125	0.064	1
MIC_{90} ($mg \cdot L^{-1}$)		1	0.5	2	0.5	1	0.25	0.25	1
Resistance, *n* (%)		0 (0)	0 (0)	0 (0)	0 (0)	0 (0)	0 (0)	0 (0)	0 (0)
Linezolid	S≤8								
MIC_{50} ($mg \cdot L^{-1}$)		1	1	1	1	1	1	2	2
MIC_{90} ($mg \cdot L^{-1}$)		2	2	2	1	1	2	4	2
Resistance, *n* (%)		0 (0)	0 (0)	0 (0)	0 (0)	0 (0)	0 (0)	0 (0)	0 (0)
Moxifloxacin	S≤1, I=2, R≥4								
MIC_{50} ($mg \cdot L^{-1}$)		1	0.5	1	0.125	1	0.064	1	0.5
MIC_{90} ($mg \cdot L^{-1}$)		2	1	1	2	4	0.25	2	0.5
Resistance, *n* (%)		1 (4.3)	0 (0)	0 (0)	0 (0)	1 (50.0)	0 (0)	0 (0)	0 (0)
Rifampin	S≤1, I=2, R≥4								
MIC_{50} ($mg \cdot L^{-1}$)		4	4	4	4	0.125	0.064	0.25	16
MIC_{90} ($mg \cdot L^{-1}$)		8	8	32	8	4	0.125	4	16
Resistance, *n* (%)		13 (56.5)	4 (57.1)	3 (60.0)	3 (75.0)	1 (50.0)	0 (0)	1 (50.0)	1 (100.0)
Tobramycin	S≤4, I=8, R≥16								
MIC_{50} ($mg \cdot L^{-1}$)		0.5	0.25	8	0.25	0.25	2	0.125	1
MIC_{90} ($mg \cdot L^{-1}$)		32	0.5	64	16	4	8	1	1
Resistance, *n* (%)		4 (17.4)	1 (14.3)	2 (40.0)	1 (25.0)	0 (0)	0 (0)	0 (0)	0 (0)
Trimethoprim-sulfamethoxazole	S≤2/38, R≥4/76								
MIC_{50} ($mg \cdot L^{-1}$)		0.25/4.75	1/19	0.125/2.375	0.125/2.375	0.25/4.75	0.25/4.75	0.125/2.375	0.25/4.75
MIC_{90} ($mg \cdot L^{-1}$)		1/19	2/38	1/19	0.25/4.75	0.25/4.75	0.25/4.75	0.5/9.5	0.25/4.75
Resistance, *n* (%)		1 (4.3)	1 (14.3)	0 (0)	0 (0)	0 (0)	0 (0)	0 (0)	0 (0)
Vancomycin	S≤2, 4≤I≤8, R≥16								
MIC_{50} ($mg \cdot L^{-1}$)		16	0.25	16	0.125	0.025	0.25	16	64
MIC_{90} ($mg \cdot L^{-1}$)		64	64	32	16	64	16	16	64
Resistance, *n* (%)		12 (52.2)	2 (28.6)	3 (60.0)	2 (50.0)	1 (50.0)	1 (50.0)	2 (100.0)	1 (100.0)

Note: I, intermediate; R, resistant; S, sensitive.

age, 14.10%), invasion (7 genes on average, 3.25%), motility (20 genes on average, 9.01%), exotoxin production (8 genes on average, 3.82%), biofilm formation (5 genes on average, 2.37%), etc. Among them, *hemB*, *hemE*, *hemH*, and *hemN* were present in almost all strains, and the *flp* genes and *hem* operons mainly encoded the adherence function of *Nocardia*. The *hly* operons and *mls* genes, which encoded hemolysin and mycolactone almost took up all the exotoxin-related genes. The presence of motility-related genes in *Nocardia* was limited, with only a small number of *flm* operons contributing to this function, and minimal variation observed among the 141 strains. The *mce* gene family, a class of genes encoding proteins involved in *Nocardia* cell invasion, had nine clusters (*mce1-9*). Among these, *mce4*, *mce5*, and *mce7* were found in the majority of *Nocardia* strains, whereas *mce1*, *mce3*, *mce6*, *mce8*, and *mce9* showed distinct distributions among the 141 strains. Interestingly, *mce2* was detected in only one strain (NBRC108239). Furthermore, six virulence genes or operons that occur with high frequency in cornea-derived *Nocardia* (*flp* genes, *glc* operon, *hly* operon, *mls* genes, *flm* operon, and *ibe* genes), but to our knowledge, these genes or operons have not been reported or comprehensively researched in other studies of *Nocardia*.

Categorization of *Nocardia* Isolated From the Cornea Based on the *mce* Gene Family

The invasion function in *Nocardia* bacteria primarily relies on the *mce* gene family. Cluster analysis of the *mce* gene family distribution categorized 23 corneal *Nocardia* strains into 3 discernible groups: group A, group B, and group C. Within group A, the *mce5A*, *mce5C*, and *mce5E* genes were consistently present in almost all strains. Group B exhibited the presence of *mce4C* and *mce4F* genes across all strains. In group C, *mce3C*, *mce4F*, and *mce5D* were detected in all strains, whereas *mce3C* was only observed within group C (Fig. 4A). Within these groups, group A included eight isolates from patients (34.8%) with mild symptoms, including *N. wallacei*, *N. asiatica*, and *N. abscessus*. Group B had seven isolates from patients (30.4%) with moderate

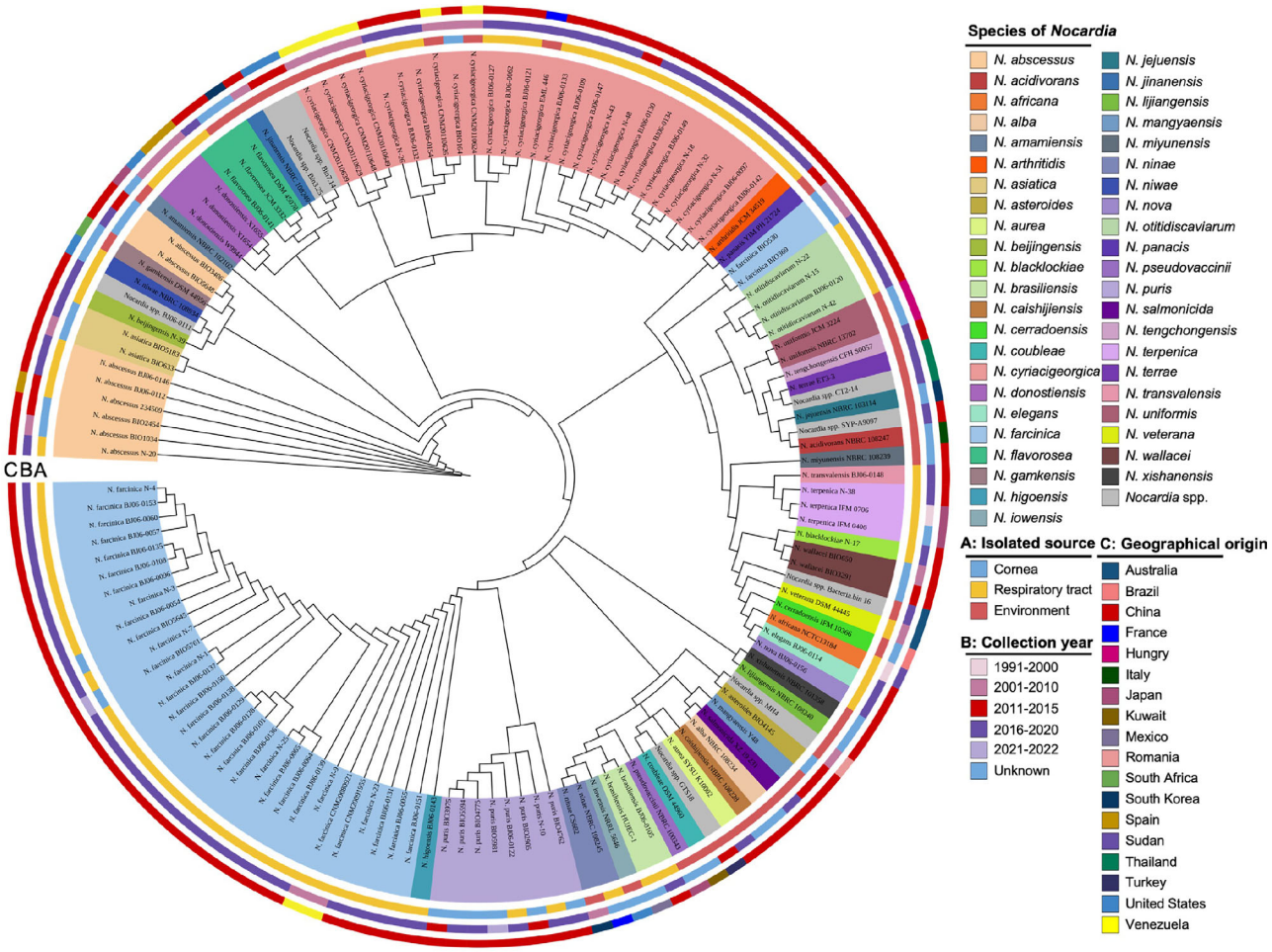

Figure 1. Whole-genome phylogenetic analysis of 141 multiple *Nocardia* strains. The innermost colored bands represent 44 different species of *Nocardia* and *Nocardia* spp. (unable to identify species). **(A)** A *colored ring* showing three different isolated sources of *Nocardia*. **(B)** A *colored ring* showing five different periods of collection years and the unknown collection years. **(C)** A colored ring showing 18 different geographic origins of *Nocardia*.

symptoms covered the species of *N. asteroids*, *N. cyriacigeorgica*, *N. puris*, and *N. farcinica*. In addition, group C comprised eight isolates from patients (34.8 %) with severe symptoms, which only belonged to *N. farcinica* and *N. puris*. Figure 4B depicted representative images of the anterior segment for each group. This distribution pattern provided insights into the specific gene variations that might contribute to the distinct characteristics of these *Nocardia* strain groups, emphasizing a potential correlation between the severity of clinical manifestations and the categorization of these groups.

Analysis of Corneal Pathogenicity Characteristics Based on Grouping With Virulence Genes

Validation of Colony Growth Characteristics of *Nocardia*. After culture on BAPs and incubated at 35°C, *Nocardia* colonies among the 3 groups were identified and their different growth patterns were photographed over a 12-hour interval (from day 0 to day 3) using slit lamp microscope and anterior segment OCT (AS-OCT; Fig. 4C). The diameter, height, and angle of the colonies were quantified and displayed in the line charts (Fig. 4D). Colonies of group A exhibited a distinctive ring-like growth pattern with a notably slower growth rate. The high-reflective signal beneath the center of the bottom in the cross-section images correlated with the thinner center of the ring seen in the slit lamp microscopy images. Group B colonies showed a mound-like shape with a smaller diameter, height, and moderate growth rate. The colonies of group C had mound-like morphology with the largest diameter (1850 ± 82.87 µm; $P = 0.0006$, versus group A; and $P < 0.0001$, versus group B), height (520 ± 13.59 µm; $P < 0.0001$, versus group A; and $P < 0.0001$, versus group B), angle (33.57 ± 0.76 degrees, $P < 0.0001$, versus group A; and $P < 0.0001$, versus group B), and fastest growth rate.

Validation of Clinical Manifestation of Mice *Nocardia* Keratitis. To assess the differences in pathogenicity of *Nocardia* keratitis after grouping based on *mce* genes, a *Nocardia* keratitis mouse model was established. Clinical scores and photographs of corneal ulcers with and without 1% sodium fluorescein were conducted at specified time points (day 1, day 3, and day 7; Fig. 5A). For the control group, mice had intact corneas with minor changes due to PBS injection on day 1. Conversely, all intervention groups exhibited evident corneal infiltrates and ulcers. In group A, on day 1, the cornea responded

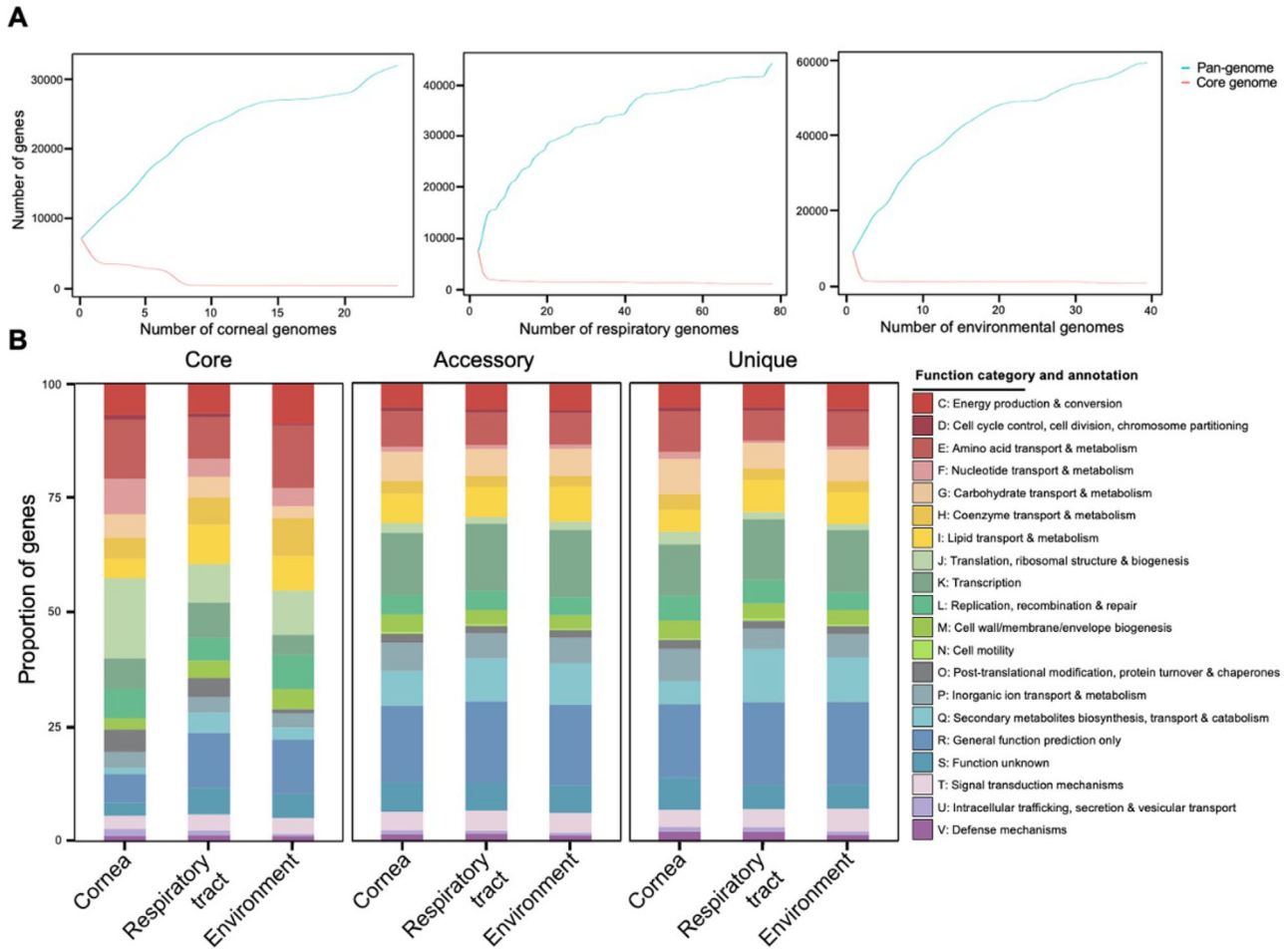

Figure 2. Pan-genome analysis of 141 multiple *Nocardia* strains grouped by three different isolated sources. (**A**) Genome size evolution curves of the pan-genome (*blue*) and core genome (*orange*) grouped by three different isolated sources. (**B**) The stacked bar chart shows the relative abundance (%) of COG categories and annotations of predicted genes within the core, accessory, and unique genomes of three isolated sources of *Nocardia*. All the categories are graphed as the percentages of the total number of genes in the core, accessory, and unique genomes.

to epithelial ulcer and moderate inflammation with dense stromal infiltrate. However, the lesion would be improved without treatment, showing a self-limited trend in the following days. In group B, the clinical manifestations and score on day 3 ($P = 0.0021$) and day 7 ($P = 0.0015$) were significantly more severe or higher than those in group A (Fig. 5B). Furthermore, the cornea response in group C was significantly more severe than those in group A and group B. On the first day, mice in group C exhibited clinical indications of corneal thinning. The inflammation steadily worsened, leading to more intense infiltration and opacity, consistent with the increasing trend of clinical scores (see Fig. 5B). For the outcome of *Nocardia* keratitis, both the size of corneal ulcers and the clinical scores increased in group C compared with the group B, with statistically significant differences (for clinical score, $P = 0.0167$; and for corneal ulcer, $P = 0.0156$; see Figs. 5B, 5C). The CFU assessment exhibited that group A had the lowest viable *Nocardia* count (3.16×10^3 CFU/mL) on day 1 post-infection, followed by group B (8.19×10^3 CFU/mL), and group C had the highest quantity (1.83×10^4 CFU/mL). The differences among the three groups are statistically significant ($F = 84.61$, $P < 0.0001$). As the observation period progressed, the bacterial count in the corneas of the three groups steadily decreased. Interestingly, by the seventh day, the mean CFU of group A had reduced to 0.56×10^3 CFU/mL, exhibiting no statistically significant difference compared to the control group (Supplementary Fig. S1).

Validation of Inflammation, Immune Reaction, and CFU of Viable Pathogen of Mice *Nocardia* Keratitis. Compared with the control group, the inflammation and immune reaction on day 7 were present with an exacerbating tendency from group A to group C. Compared to the control group, the mean number of cells staining with H&E were 242.00 cells per field ($P = 0.0378$), 449.33 cells per field ($P < 0.0001$), and 621 cells per field ($P < 0.0001$), the mean relative optical density of IFN-γ was 2.74 folds ($P = 0.0019$), 3.53 folds ($P = 0.0001$), and 4.17 folds ($P < 0.0001$), and the mean count of CD4+ cells were 2.00 cells per field ($P = 0.2503$), 4.67 cells per field ($P = 0.0032$), and 8.33 cells per field ($P < 0.0001$), which both exhibited ascending trends from group A to group C. This effect was particularly pronounced in the corneal stroma, aligning with the outcomes of histological examination and clinical presentation. The relative expression levels of IL-6Rα and TNF-

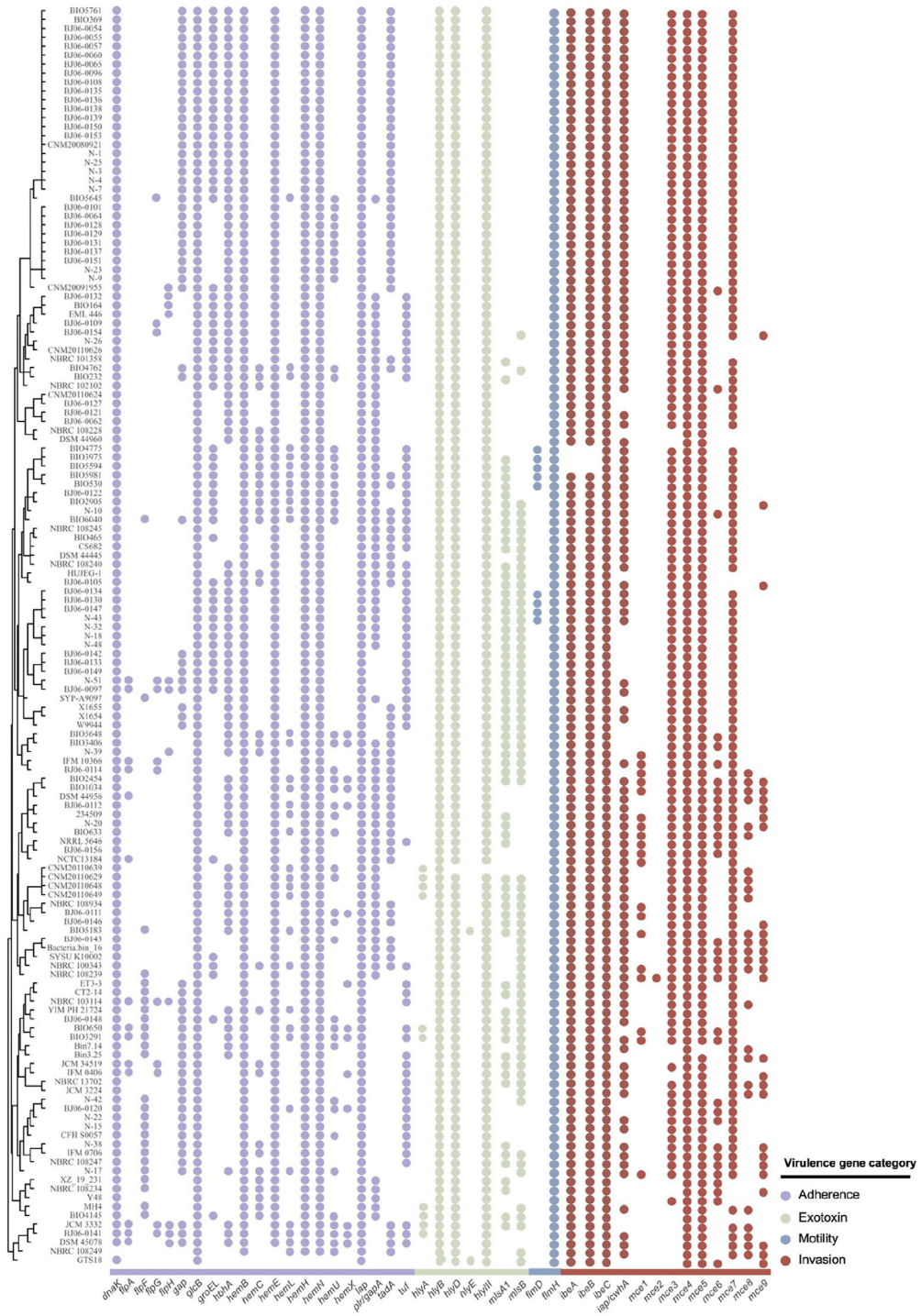

Figure 3. Distribution of four typical virulence factor categories within the whole genome of 141 multiple *Nocardia* strains. Each dot represents the presence of a virulence factor. Four colors (*violet*, *green*, *blue*, and *red*) correspond to four virulence factor categories (adherence, exotoxin, motility, and invasion), respectively.

α demonstrated analogous patterns to the aforementioned biomarkers. For example, the mean relative expression levels of IL-6Rα in groups A, B, and C were 2.28 folds ($P = 0.0086$), 2.90 folds ($P = 0.0006$), and 3.89 folds ($P < 0.0001$), respectively, and the mean relative expression levels of TNF-α were 1.69 folds ($P = 0.0116$), 2.44 folds ($P < 0.0001$), and 3.72 folds ($P < 0.0001$), respectively (Fig. 6).

Analysis of Antibiotic Resistance Genes Among the *Nocardia* Isolated From the Cornea

To detect antibiotic resistance properties of *Nocardia* at the genomic level, ARGs were identified by BLASTp against CARD. These ARGs spanned nine distinct drug classes, four resistance mechanisms, and seven primary AMR gene fami-

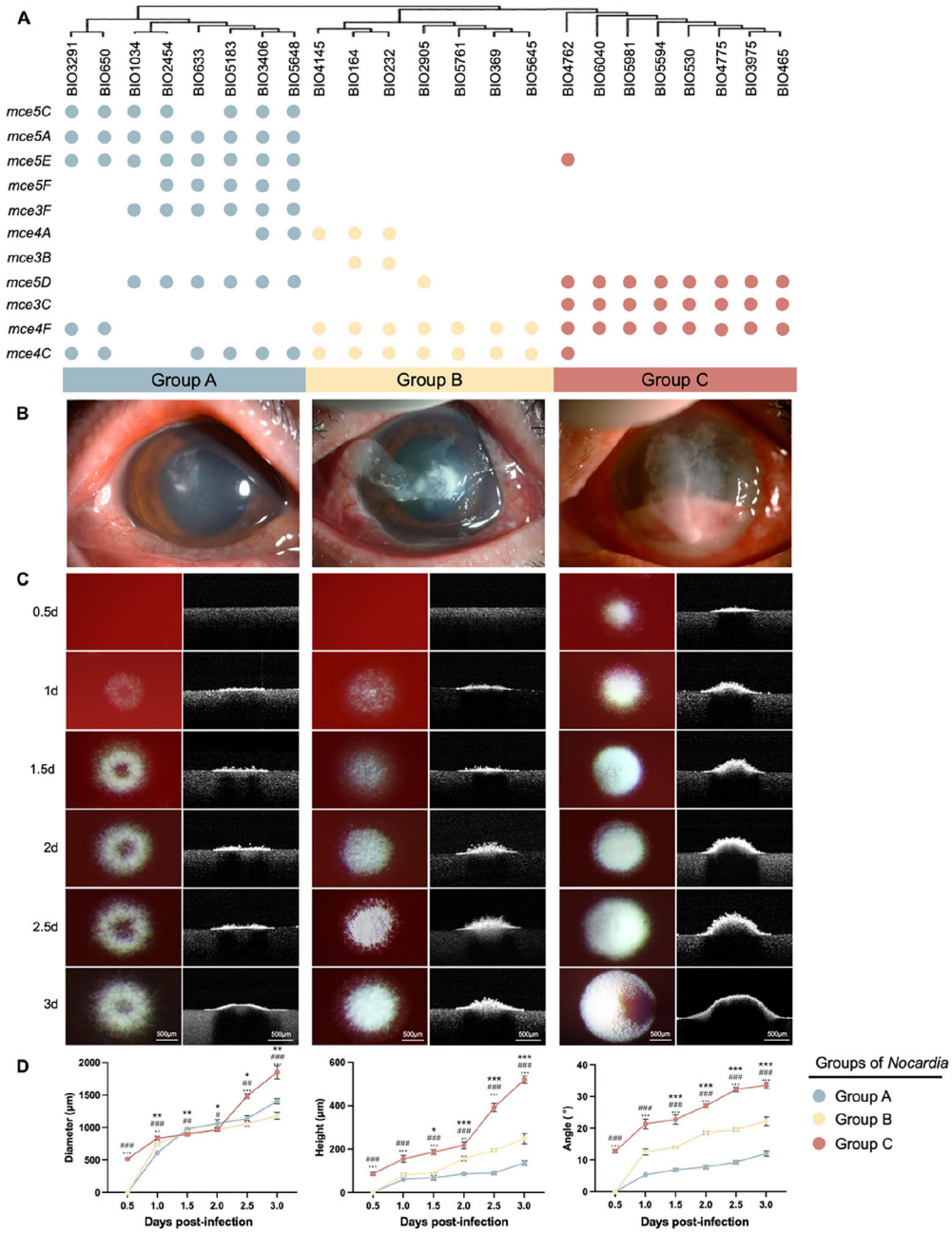

Figure 4. Twenty-three strains of *Nocardia* isolated from the cornea can be categorized into three groups. (**A**) Twenty-three strains of *Nocardia* were grouped based on the distribution of the *mce* gene family. Each *dot* represents the presence of a *mce* gene. (**B**) The representative anterior segment photographs of patients with *Nocardia* keratitis correspond to three different groups. (**C**) The representative slit lamp microscopic and AS-OCT images of *Nocardia* colonies on BAP media correspond to three different groups ($n = 3$). The morphological changes were observed and photographed at 0.5, 1, 1.5, 2, 2.5, and 3 days post-infection. (**D**) The increasing trends of diameter, height, and angle in three groups of *Nocardia* ($n = 3$). One-way ANOVA followed by Tukey post hoc tests were performed to assess differences among three groups of *Nocardia* at the same incubation time (***$P < 0.001$, **$P < 0.01$, *$P < 0.05$, group A versus group B; ###$P < 0.001$, ##$P < 0.01$, #$P < 0.05$, group A versus group C; …, $P < 0.001$, …, $P < 0.01$, …, $P < 0.05$, group B versus group C).

lies. Table 3 presents the average gene length and distribution of these ARGs. Particularly noteworthy, the vancomycin resistance gene family covered every strain isolated from the cornea. Among them, *vanB*, *vanI*, and *vanG* were the most widely distributed. Moreover, the rifampin resistance gene family (*rox-sv* and *rox-nf*) covered 87.0% of the corneal isolated strains (20 strains).

Discussion

In this study, whole genome sequencing was performed on 23 *Nocardia* strains isolated from the cornea in the current cohort. The objective was to gain a thorough understanding of the phylogenetic relationship among *Nocardia* strains from different sources, including the cornea,

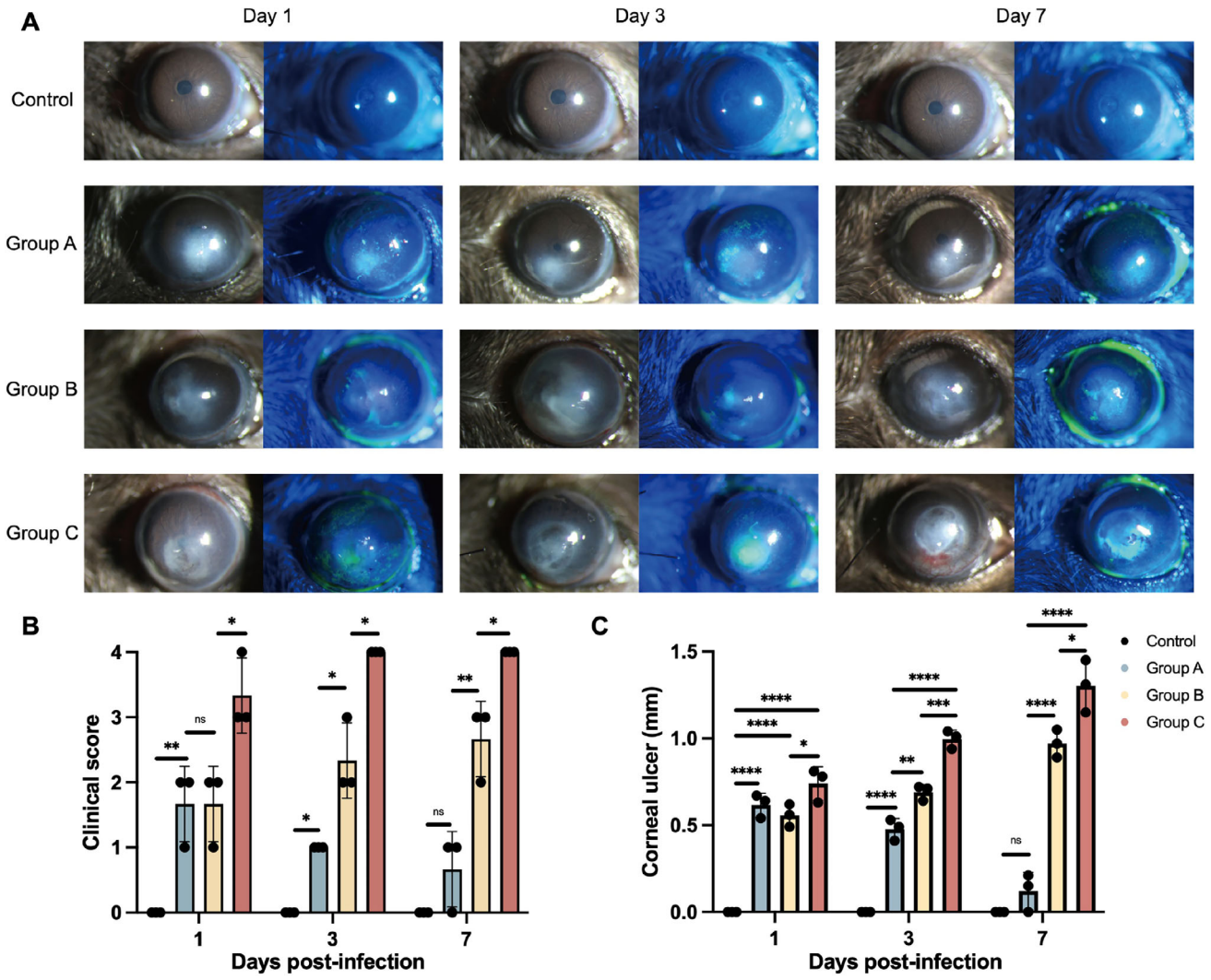

Figure 5. The anterior segment photographs and clinical scores of *Nocardia* keratitis model mice in four groups (control group, group A, group B, and group C). (**A**) The representative anterior segment photographs with and without fluorescein staining under slit lamp microscopy on days 1, 3, and 7 ($n = 3$). (**B**) The clinical scores and (**C**) the diameters of the corneal ulcers were assessed in each group, and three mice were assessed in each group for the indicated time ($n = 3$). One-way ANOVA followed by Tukey post hoc tests were performed to assess differences between four groups of *Nocardia* at the same time post-infection (****$P < 0.0001$; ***$P < 0.001$; **$P < 0.01$; *$P < 0.05$; ns, no significance).

respiratory tracts, and environment, as well as to explore the similarities and differences in their biological functions and virulence properties. As a vital virulence factor in *Nocardia* strains isolated from the cornea, the *mce* gene family was also further investigated. The distinct distribution of *mce* genes led to the categorization of cornea-derived *Nocardia* strains into three groups. The accuracy of this categorization was verified by in vitro analysis of strain growth patterns and in vivo testing using a *Nocardia* keratitis mouse model. The model was assessed using clinical scores and various histopathologic analyses, including H&E staining, immunochemistry, and immunofluorescence staining with specific biomarkers (CD4, IFN-γ, IL-6Rα, and TNF-α). To date, it was the largest series with *Nocardia* keratitis on clinical profiles and pathogenetic grouping based on WGS. Additionally, the study involved an analysis of antimicrobial susceptibility testing and ARGs to detect the unique antimicrobial resistance properties of the *Nocardia* strains in this particular cohort.

In this cohort, *Nocardia* keratitis had a longer mean presentation time (20.50 ± 2.86 days) and resolution time (33.00 ± 7.07 days) compared to other forms of bacterial or infectious keratitis (4.0–14.0 days[31–33] and 5.8–14.0 days[33–35]), and consistent with the previous cohorts of *Nocardia* keratitis.[36,37] Among the various strains, *N. puris* was the most common isolate, followed by *N. abscessus*, *N. cyriacigeorgica*, and *N. farcinica*. Despite the genetic similarities observed among the corneal *Nocardia* isolates, there were variations in terms of antimicrobial resistance properties of the strains, the clinical characteristics, severity, and outcomes of *Nocardia* keratitis. Notably, all strains showed sensitivity to amikacin, imipenem, and linezolid. However, apart from *N. puris*, over half of the strains within each species were resistant to vancomycin. Furthermore, 13 strains displayed resistance to rifampin, showcasing peculiar

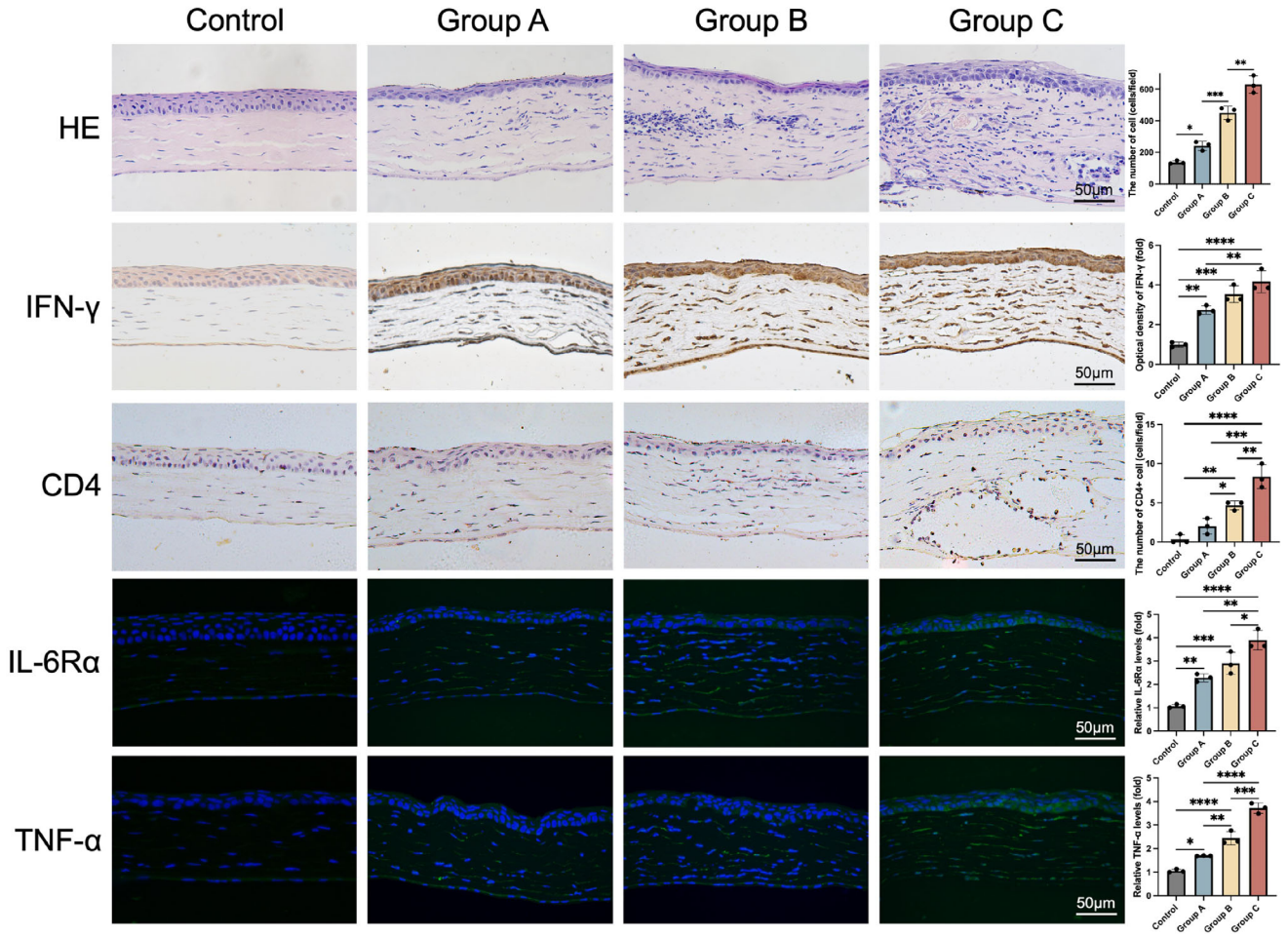

Figure 6. Histological analysis and detection of CD4+ cells, IFN-γ, IL-6Rα, and TNF-α expression in the cornea of *Nocardia* keratitis mouse model. Representative images of histological analysis by H&E staining revealed the presence of epithelial, stromal, endothelial, and inflammatory cells in the control group and three intervention groups. Representative images of immunohistochemistry (IHC) staining of IFN-γ and CD4+ cells, immunofluorescence (IF) staining of IL-6Rα and TNF-α reveal the inflammation in the cornea of *Nocardia* keratitis mouse model ($n = 3$). The results were plotted as the number of cells stained with H&E, positive cells per field (CD4), or fold changes compared with the control group (IFN-γ, IL-6Rα, and TNF-α). Three fields of view per section were selected for mean value calculation and statistical analysis (****$P < 0.0001$, ***$P < 0.001$, **$P < 0.01$, *$P < 0.05$). Scale bar, 50 μm.

Table 3. The Antibiotic Resistance Genes Within the Whole Genome of 23 Strains of *Nocardia* Isolated From the Cornea

Drug Class	Resistance Mechanism	Main AMR Gene Family	Average Gene Length (±SD) (bp)	ARGs (The Number of Strains Included)
Cephalosporin	Antibiotic inactivation	Beta-lactamase	932	*ast-1* (2)
Diaminopyrimidine antibiotic	Antibiotic target alteration	Trimethoprim resistant dihydrofolate reductase	485	*dfrC* (1)
Disinfecting agents and antiseptics	Antibiotic efflux	Small multidrug resistance (SMR) antibiotic efflux pump	386 ± 63	*qacG* (2), *sepA* (1)
Fluoroquinolone antibiotic	Antibiotic efflux	Major facilitator superfamily (MFS) antibiotic efflux pump	1086 ± 381	*mgrA* (1), *norA* (1), *norC* (1), *sdrM* (1)
Glycopeptide antibiotic	Antibiotic target alteration	Glycopeptide resistance gene cluster	1105 ± 901	*vanA* (1), *vanB* (22), *vanF* (1), *vanG* (8), *vanI* (22), *vanM* (2), *vanO* (1)
Monobactam	Antibiotic inactivation	Beta-lactamase	860	$bla_{TEM\text{-}116}$ (1)
Penam	Antibiotic inactivation	Beta-lactamase	893 ± 30	*blaZ* (1), *far-1* (4)
Rifamycin antibiotic	Antibiotic inactivation	Rifampin monooxygenase	1429 ± 7	*rox-nf* (5), *rox-sv* (16), *rpoB2* (2)
Salicylic acid antibiotic	Antibiotic target alteration	Aminosalicylate resistant dihydrofolate synthase	1451	*folC* (1)

Note: AMR, antimicrobial resistance; ARGs, antimicrobial resistance genes.

antimicrobial resistance profiles that differed from previous studies.[36–38]

Combining with the whole genome sequences online, most of the same species of 141 strains of *Nocardia* from different sources were harbored in the same clade suggesting the accuracy and precision of our whole-genome phylogenetic analysis. Among the strains studied, 32 of 34 strains of *N. farcinica* and all strains of *N. puris* were isolated from China, suggesting certain species of *Nocardia* were restricted in specific regions with the influence of climate and environmental factors.[39] The pan-genome analysis focused on the collective set of genes found across all strains and revealed that the pan-genomes of *Nocardia* from all three sources were "open," which means that these *Nocardia* strains have the capacity to colonize and exploit various environmental niches. This adaptability is likely achieved through horizontal gene transfer,[40] allowing them to acquire new genetic material and the capacity to survive in a complicated host environment.[41] The distinctive functional distribution among COG indicated the characteristic living patterns of *Nocardia* from different isolated sources, which were assigned to multiple categories. Especially for core and accessory genomes of *Nocardia*, the gene cluster functioning as cell wall/membrane/envelope biogenesis (category M), displayed significant differences between corneal and environmental isolates.

Unlike environmentally isolated *Nocardia*, the cornea-derived *Nocardia* needed to interact with and invade corneal tissue, therefore, had the possibility that categories M-related genes hold associations with the virulence of *Nocardia*, potentially playing a pivotal role in the onset and progression of *Nocardia* keratitis. In this study, a mean of 220 virulence factors and corresponding virulence genes were detected, which played crucial roles in regulating the initiation and progression of *Nocardia* infection. For *Nocardia* isolated from the cornea, virulence genes predominantly contributed to the pathogenesis of the strains and interactions between host and pathogen, such as adherence, invasion, motility, exotoxin production, biofilm formation, etc. After adherence to host cells, invasion is the key pathogenetic process of *Nocardia* keratitis.[42] For genes among them, the *mce* gene family is a cell wall-related protein, which has an association with category M in COG and is proven to have crucial effects on the invasive process of *Nocardia*,[43] especially into the cornea and their survival in phagocytes, epithelial cells, under hypoxic condition.[44–48] Because *mce4*, *mce5*, and *mce7* were found in the majority of *Nocardia* strains, *mce1*, *mce3*, *mce6*, *mce8*, and *mce9* showed distinct distributions. In addition, every cluster of *mce* gene had multiple genes involved (normally from A to F), these provided a basis for grouping based on the distribution of the *mce* gene family.

For the peculiar distribution of specific *mce* genes, within group A, the *mce5A*, *mce5C*, and *mce5E* genes were consistently present in almost all strains and potentially played a critical role in the invasion of host cells under hypoxic conditions however further research is needed.[49] All strains across group B displayed the presence of *mce4C* and *mce4F* genes with multiple pathogenic effects which were well-studied. For encoding a cholesterol transporter,[50,51] *mce4* contributes to the entrance of *Nocardia* into a tryptophan aspartate-containing coat protein (TACO) – coated phagosomes to prevent the degradation of lysosomes,[52] meanwhile promoting the localization and invasion of *Nocardia* to host cells through cholesterol-rich domains of the plasma membrane.[53,54] Furthermore, *mce4C* and *mce4F* genes allow *Nocardia* to grow under hypoxic conditions, by taking in cholesterol as a carbon source, therefore, providing energy for *Nocardia* survival inside the cornea and deeper invasion.[48] All strains in group C contained the *mce4F* gene, thus obtaining similar basic pathogenic properties to group B. *Mce4F*, an essential component of the *mce4* operon, is found in the genomes of mycobacteria and *Nocardia*.[55] *Mce4F* encodes external membrane proteins, crucial for bacterial pathogenesis.[56] This study indicates the highly conservation of *mce4F* across various *Nocardia* strains, making it a valuable and reliable diagnostic marker, especially for early detection, saving time compared to the culture method. Additionally, Kendall et al.[57] demonstrated that the KstR|Rv3574 transcriptional regulon controls *mce4F* expression through lipid catabolism, vital for bacterial survival. Therefore, *mce4F* shows promise as a potential therapeutic target for combating these infections. Remarkably, the *mce3C* gene was only detected in the strains of *Nocardia* in group C, which triggered the immune escape by promoting *Nocardia* to invade and survive within macrophages and other inflammatory cells.[47,58] The ubiquitous presence of *mce3C* within group C might be the cause of poor clinical manifestations and outcomes of the patients and also can be the biomarker to evaluate the prognosis of *Nocardia* keratitis, especially in the early stage of the disease.

In previous studies, Mce proteins were suggested as diagnosis markers for various mycobacterial infections.[54,59,60] However, specific *mce* gene (such as *mce3C*, *mce4C*, *mce4F*, etc.) that can be easily detected using polymerase chain reaction (PCR) has not been proposed yet. Interestingly, distinct growth patterns were observed among the three groups of *Nocardia* strains, and these were confirmed using slit lamp microscopy and AS-OCT. The appearance of the colonies also differed: group A exhibited a distinctive ring-like colony, whereas groups B and C were mound-like. The growth rate increased significantly from group A to group C, as evident from trends in colony diameter, height, and angle. Furthermore, the growth pattern of *Nocardia* colonies might correlate with the clinical manifestations, especially the ring-like colony of group A, whose patients' lesions showed wreath-like infiltration. Additionally, the rate of Nocardia colony growth was linked to patient outcomes. Group C, with the fastest growth rate, had a higher proportion of patients in the cohort requiring therapeutic keratoplasty, indicating worse outcomes.

The phenotypes of *Nocardia* keratitis corresponded to genotype-based groupings of *Nocardia* strains isolated from the patients. In group A, *Nocardia* keratitis is milder and self-limiting, with clinical scores and corneal ulcer tapering off and ending up with corneal scarring formation on day 7. Group B presented moderate course and outcomes with relatively slow progression, whereas group C initiated with acute onset in one day and exacerbated in the following week, resulting in central corneal thinning and perforation in some of the mouse models. The results of CFU assessment were consistent with clinical outcomes, with mice in group A having the lowest CFU, group B the next highest, and group C the most. The total amount of *Nocardia* isolated from the cornea was reduced in all three groups, which was mainly a result of the immune response to the infection and thus killing the pathogen. Compared to the control group, H&E staining exhibited an increasing trend of inflammatory cell activation in the lesion area. IFN-γ, a pro-inflammatory cytokine produced

Investigative Ophthalmology & Visual Science

by various inflammatory cells (neutrophils, macrophages, B lymphocytes, and T lymphocytes, etc.).[61] The relative OD value of IFN-γ also reflects the exacerbation of inflammation condition, especially in the corneal stroma which corresponded to the extent of corneal infiltration and opacity in the animal model. Previous studies demonstrated that IL-6R was essential to the immune response,[62] furthermore, IL-6Rα as the main functional subunit of IL-6R,[63] acted as the key protein in the signal pathway for driving naive CD4+ T cells to the Th17 lineage T cells (mature CD4+ T cells) by dendritic cells.[64] Thus, *Nocardia* infection triggered the immune response in the cornea and upregulated the expression level of IL-6R, as well as IL-6Rα, further promoting the maturation of CD4+ cells to Th17 lineage T cells with an increasing trend from group A to group C, which was validated by immunofluorescence staining in the current study. In addition, the mononuclear phagocyte system (MPS) was also activated by *Nocardia* infection in identical trends, as the positive staining of TNF-α, which was primarily released by MPS.[65]

The ARGs among 23 cornea-derived *Nocardia* were eventually detected. Similar to the antimicrobial susceptibility testing, the ARGs of two powerful antibiotics, vancomycin and rifampin widely distributed, differing from previous clinical strains[66] and the isolates from respiratory tracts and environment (Supplementary Fig. S2), which probably was the result of horizontal gene transfer and topical antibiotic therapy. Moreover, clusters *vanB* and *vanI* contributed to the mainstay of the vancomycin resistance gene, which varied from other vancomycin-resistant bacteria.[67–70] Of the 122 downloaded *Nocardia* strains, 27 had antibiotic susceptibility test results (Supplementary Table S1). Among the 10 antibiotics included in this study, there was no significant difference in the susceptibility of cornea-derived *Nocardia* to the four antibiotics (i.e., amikacin, ceftriaxone, moxifloxacin, and tobramycin) when compared with non-cornea-derived *Nocardia*; significantly higher susceptibility to clarithromycin ($P < 0.001$), imipenem ($P < 0.001$), linezolid ($P < 0.05$), and methotrexate-sulfamethoxazole ($P < 0.01$); and significantly lower susceptibility and resistance to rifampin ($P < 0.05$) and vancomycin ($P < 0.05$), which was generally consistent with the results of resistance gene analysis.

Our study still had several limitations. First, the bioinformatics methods were mainly used to detect the presence of specific genes in *Nocardia* strains. Although the algorithms of those were proven accurate and reliable, it would be better to validate the *mce* gene family distribution in vivo on nucleic acid levels with molecular biological methods. Second, due to a rather rare ocular infection and its relatively low incidence, the cohort of patients with *Nocardia* keratitis was relatively limited in size. It would be advantageous to construct a prospective cohort study involving a larger number of patients. This expanded cohort would provide more comprehensive data for further research and a better understanding of *Nocardia* keratitis. Third, although based on the practical considerations, only female mice were involved in these animal experiments. Further studies with both male and female mice would reduce the gender bias and enhance the understanding of *Nocardia* keratitis classification. At last, this study only proposed a categorization of cornea-derived *Nocardia* based on the distribution of the *mce* gene family, however, more research focusing on the pathogenesis of *Nocardia* keratitis is needed.

In summary, our study has provided valuable insights into the profile of virulence and antimicrobial resistance genes among various *Nocardia* strains. This has enhanced our comprehension of *Nocardia* keratitis and offered guidance for improved diagnosis and treatment strategies. By using whole genome sequencing, we have underscored the significance of the *mce* gene family in genotype-based classification to *Nocardia* keratitis.

Acknowledgments

Supported by grants from the National Key Research and Development Program of China (2021YFC2301000).

Disclosure: **X. Guo**, None; **Z. Zhang**, None; **Q. Chen**, None; **L. Wang**, None; **X. Xu**, None; **Z. Wei**, None; **Y. Zhang**, None; **K. Chen**, None; **Z. Wang**, None; **X. Lu**, None; **Q. Liang**, None

References

1. Meier-Kolthoff JP, Carbasse JS, Peinado-Olarte RL, Goker M. TYGS and LPSN: a database tandem for fast and reliable genome-based classification and nomenclature of prokaryotes. *Nucleic Acids Res.* 2022;50(D1):D801–D807.
2. Beaman BL, Beaman L. *Nocardia* species: host-parasite relationships. *Clin Microbiol Rev.* 1994;7(2):213–264.
3. Zhang J, Zhu Y, Sun Y, Han X, Mao Y. Pathogenic Nocardia amamiensis infection: a rare case report and literature review. *Heliyon.* 2023;9(7):e17183.
4. Conville PS, Brown-Elliott BA, Smith T, Zelazny AM. The complexities of *Nocardia* taxonomy and identification. *J Clin Microbiol.* 2017;56(1):e01419–e01417.
5. Lalitha P. *Nocardia* keratitis. *Curr Opin Ophthalmol.* 2009; 20(4):318–323.
6. Brown-Elliott BA, Brown JM, Conville PS, Wallace RJ, Jr. Clinical and laboratory features of the Nocardia spp. based on current molecular taxonomy. *Clin Microbiol Rev.* 2006;19(2):259–282.
7. Hau SC, Dart JK, Vesaluoma M, et al. Diagnostic accuracy of microbial keratitis with in vivo scanning laser confocal microscopy. *Br J Ophthalmol.* 2010;94(8):982–987.
8. Chang EL, Chu RL, Wittpenn JR, Perry HD. Nocardia keratitis mimicking superior limbic keratoconjunctivitis and herpes simplex virus. *Am J Ophthalmol Case Rep.* 2021;22:101030.
9. Lalitha PTM, Prajna NV, Gilpin C, Prakash K, Srinivasan M. Nocardia keratitis species, drug sensitivities, and clinical correlation. *Cornea.* 2007;26(3):255–259.
10. Balloux F, Bronstad Brynildsrud O, van Dorp L, et al. From theory to practice: translating whole-genome sequencing (WGS) into the clinic. *Trends Microbiol.* 2018;26(12):1035–1048.
11. Boolchandani M, D'Souza AW, Dantas G. Sequencing-based methods and resources to study antimicrobial resistance. *Nat Rev Genet.* 2019;20(6):356–370.
12. Acharya M, Farooqui JH, Jain S, Mathur U. Pearls and paradigms in infective keratitis. *Romanian J Ophthalmol.* 2019;63(2):119–127.
13. Clinical and Laboratory Standards Institute. 13th ed. *CLSI standard M02.* Wayne, PA: Clinical and Laboratory Standards Institute; 2018. pp. 19–21.
14. Kralik P, Beran V, Pavlik I. Enumeration of Mycobacterium avium sub sp. paratuberculosis by quantitative real-time PCR, culture on solid media and optical densitometry. *BMC Res Notes.* 2012; 5: 114.
15. Forbes BA, Sahm DF, Weissfeld AS. Bailey & Scott's Diagnostic Microbiology. Eleventh Edition. St. Louis, MO: Mosby Inc; 2002. *Laboratory methods for detection of antibacterial resistance*; pp. 230–231.

16. Prjibelski A, Antipov D, Meleshko D, Lapidus A, Korobeynikov A. Using SPAdes de novo assembler. *Curr Protoc Bioinformatics.* 2020;70(1):e102.
17. Seemann T. Prokka: rapid prokaryotic genome annotation. *Bioinformatics.* 2014;30(14):2068–2069.
18. Gurevich A, Saveliev V, Vyahhi N, Tesler G. QUAST: quality assessment tool for genome assemblies. *Bioinformatics.* 2013;29(8):1072–1075.
19. Chaumeil PA, Mussig AJ, Hugenholtz P, Parks DH. GTDB-Tk v2: memory friendly classification with the genome taxonomy database. *Bioinformatics.* 2022;38(23):5315–5316.
20. Letunic I, Bork P. Interactive Tree Of Life (iTOL) v5: an online tool for phylogenetic tree display and annotation. *Nucleic Acids Res.* 2021;49(W1):W293–W296.
21. Petit RA, 3rd, Read TD. Bactopia: a flexible pipeline for complete analysis of bacterial genomes. *mSystems.* 2020;5(4):e00190–20.
22. Chaudhari NM, Gupta VK, Dutta C. BPGA - an ultra-fast pan-genome analysis pipeline. *Sci Rep.* 2016;6:24373.
23. Tatusov RL, Natale DA, Garkavtsev IV, et al. The COG database: new developments in phylogenetic classification of proteins from complete genomes. *Nucleic Acids Res.* 2001;29(1):22–28.
24. Liu B, Zheng D, Zhou S, Chen L, Yang J. VFDB 2022: a general classification scheme for bacterial virulence factors. *Nucleic Acids Res.* 2022;50(D1):D912–D917.
25. Alcock BP, Huynh W, Chalil R, et al. CARD 2023: expanded curation, support for machine learning, and resistome prediction at the Comprehensive Antibiotic Resistance Database. *Nucleic Acids Res.* 2023;51(D1):D690–D699.
26. Chojnacki M, Philbrick A, Wucher B, et al. Development of a broad-spectrum antimicrobial combination for the treatment of Staphylococcus aureus and Pseudomonas aeruginosa corneal infections. *Antimicrob Agents Chemother.* 2018;63(1): e01929–e18.
27. Alionte LG, Cannon BM, White CD, et al. Hobden. Pseudomonas aeruginosa LasA protease and corneal infections. *Curr Eye Res.* 2001; 22(4): 266–271.
28. Zhang Y, Zhou N, Jiao Y, et al. Targeting noncanonical pyroptosis with a small molecular inhibitor alleviates inflammation in the LPS-induced keratitis mouse model. *Invest Ophthalmol Vis Sci.* 2023;64(1):1.
29. Ucgul AY, Behcet M. Comparison of the effect of teicoplanin and vancomycin on experimental methicillin-resistant staphylococcus aureus keratitis. *Int Ophthalmol.* 2021;41(4):1395–1402.
30. Hazlett LD, Moon MM, Strejc M, Berk RS. Evidence for N-acetylmannosamine as an ocular receptor for P. aeruginosa adherence to scarified cornea. *Invest Ophthalmol Vis Sci.* 1987;28:1978–1985.
31. Atta S, Perera C, Nayyar S, Kowalski RP, Jhanji V. An 18-year overview of Serratia marcescens ocular infection. *Eye Contact Lens.* 2021;47(8):471–475.
32. Durrani AF, Atta S, Bhat AK, et al. Methicillin-resistant *Staphylococcus aureus* keratitis: initial treatment, risk factors, clinical features, and treatment outcomes. *Am J Ophthalmol.* 2020;214:119–126.
33. Chantra S, Jittreprasert S, Chotcomwongse P, Amornpetchsathaporn A. Estimated direct and indirect health care costs of severe infectious keratitis by cultured organisms in Thailand: an 8-year retrospective study. *PLoS One.* 2023;18(7):e0288442.
34. Wong TOS, Gamble G, McGhee CN. Severe infective keratitis leading to hospital admission in New Zealand. *Br J Ophthalmol.* 2003;87(9):1103–1108.
35. Ting DSJ, Cairns J, Gopal BP, et al. Risk factors, clinical outcomes, and prognostic factors of bacterial keratitis: the Nottingham Infectious Keratitis Study. *Front Med (Lausanne).* 2021;8:715118.
36. Adre E, Maestre-Mesa J, Durkee H, et al. Nocardia keratitis: amikacin nonsusceptibility, risk factors, and treatment outcomes. *J Ophthalmic Inflamm Infect.* 2022;12(1): 11.
37. DeCroos FC, Garg P, Reddy AK, et al. Optimizing diagnosis and management of Nocardia keratitis, scleritis, and endophthalmitis: 11-year microbial and clinical overview. *Ophthalmology.* 2011;118(6):1193–1200.
38. Reddy AK, Garg P, Kaur I. Spectrum and clinicomicrobiological profile of Nocardia keratitis caused by rare species of Nocardia identified by 16S rRNA gene sequencing. *Eye (Lond).* 2010;24(7):1259–1262.
39. Rafiei N, Peri AM, Righi E, Harris P, Paterson DL. Central nervous system nocardiosis in Queensland: a report of 20 cases and review of the literature. *Medicine (Baltimore).* 2016;95(46):e5255.
40. Tettelin HMV, Cieslewicz MJ, Donati C, et al. Genome analysis of multiple pathogenic isolates of Streptococcus agalactiae: implications for the microbial "pan-genome". *Proc Natl Acad Sci USA.* 2005;102(39):13950–13955.
41. De Maayer PCW, Rubagotti E, Venter SN, Toth IK, Birch PR, Coutinho TA. Analysis of the Pantoea ananatis pan-genome reveals factors underlying its ability to colonize and interact with plant, insect, and vertebrate hosts. *BMC Genomics.* 2014;15(1):404.
42. Luo M, Zhang X, Zhang S, et al. Crystal structure of an invasivity-associated domain of SdrE in S. aureus. *PLoS One.* 2017;12(1):e0168814.
43. Lim J, Park HT, Ko S, et al. Genomic diversity of Mycobacterium avium subsp. Paratuberculosis: pangenomic approach for highlighting unique genomic features with newly constructed complete genomes. *Vet Res.* 2021;52(1):46.
44. Ji X, Tan X, Hou X, et al. Cloning, expression, invasion, and immunological reactivity of a mammalian cell entry protein encoded by the mce1 operon of Nocardia farcinica. *Front Microbiol.* 2017;8:281.
45. Ji X, Zhang X, Sun L, et al. Mce1C and Mce1D facilitate N. farcinica invasion of host cells and suppress immune responses by inhibiting innate signaling pathways. *Sci Rep.* 2020;10(1):14908.
46. Xu S, Wei M, Li G, et al. Comprehensive analysis of the Nocardia cyriacigeorgica complex reveals five species-level clades with different evolutionary and pathogenicity characteristics. *mSystems.* 2022;7(3):e0140621.
47. Zhang Y, Li J, Li B, Wang J, Liu CH. Mycobacterium tuberculosis Mce3C promotes mycobacteria entry into macrophages through activation of β2 integrin-mediated signalling pathway. *Cell Microbiol.* 2018;20(2):e12800.
48. Rathor N, Garima K, Sharma NK, Narang A, Varma-Basil M, Bose M. Expression profile of mce4 operon of Mycobacterium tuberculosis following environmental stress. *Int J Mycobacteriol.* 2016;5(3):328–332.
49. Jiang J, Lin C, Zhang J, et al. Transcriptome changes of Mycobacterium marinum in the process of resuscitation from hypoxia-induced dormancy. *Front Genet.* 2019;10:1359.
50. Liu D, Hao K, Wang W, et al. Rv2629 overexpression delays Mycobacterium smegmatis and Mycobacteria tuberculosis entry into log-phase and increases pathogenicity of Mycobacterium smegmatis in mice. *Front Microbiol.* 2017;8:2231.
51. VanderVen BC, Huang L, Rohde KH, Russell DG. The minimal unit of infection*: mycobacterium tuberculosis* in the macrophage. *Microbiol Spectr.* 2016;4(6), doi:10.1128/microbiolspec.TBTB2-0025-2016.
52. Gatfield J, Pieters J. Essential role for cholesterol in entry of mycobacteria into macrophages. *Science.* 2000;288(5471):1647–1650.

Investigative Ophthalmology & Visual Science

53. Tanigawa K, Hayashi Y, Hama K, et al. Mycobacterium leprae promotes triacylglycerol *de novo* synthesis through induction of GPAT3 expression in human premonocytic THP-1 cells. *PLoS One.* 2021;16(3):e0249184.
54. Perkowski EF, Miller BK, McCann JR, et al. An orphaned Mce-associated membrane protein of Mycobacterium tuberculosis is a virulence factor that stabilizes Mce transporters. *Mol Microbiol.* 2016;100(1):90–107.
55. Song H, Sandie R, Wang Y, et al. Identification of outer membrane proteins of Mycobacterium tuberculosis. *Tuberculosis (Edinb).* 2008;88:526–544.
56. Joshi SM, Pandey AK, Capite N, et al. Characterization of mycobacterial virulence genes through genetic interaction mapping. *Proc Natl Acad Sci USA.* 2006;103:11760–11765.
57. Kendall SL, Withers M, Soffair CN, et al. A highly conserved transcriptional repressor controls a large regulon involved in lipid degradation in Mycobacterium smegmatis and Mycobacterium tuberculosis. *Mol Microbiol.* 2007;65:684–699.
58. Fenn K, Wong CT, Darbari VC. Mycobacterium tuberculosis uses Mce proteins to interfere with host cell signaling. *Front Mol Biosci.* 2019;6:149.
59. Mikheecheva NE, Zaychikova MV, Melerzanov AV, Danilenko VN. A nonsynonymous SNP catalog of Mycobacterium tuberculosis virulence genes and its use for detecting new potentially virulent sublineages. *Genome Biol Evol.* 2017;9(4):887–899.
60. Khan S, Islam A, Hassan MI, Ahmad F. Purification and structural characterization of Mce4A from Mycobacterium tuberculosis. *Int J Biol Macromol.* 2016;93(Pt A):235–241.
61. Lin YJ, Anzaghe M, Schulke S. Update on the pathomechanism, diagnosis, and treatment options for rheumatoid arthritis. *Cells.* 2020;9(4):880.
62. Sarsu SB, Yilmaz SG, Bayram A, et al. Polymorphisms in the IL-6 and IL-6R receptor genes as new diagnostic biomarkers of acute appendicitis: a study on two candidate genes in pediatric patients with acute appendicitis. *Ital J Pediatr.* 2015;41:100.
63. Gruol DL, Melkonian C, Huitron-Resendiz S, Roberts AJ. Alcohol alters IL-6 signal transduction in the CNS of transgenic mice with increased astrocyte expression of IL-6. *Cell Mol Neurobiol.* 2021;41(4):733–750.
64. Heink S, Yogev N, Garbers C, et al. Trans-presentation of IL-6 by dendritic cells is required for the priming of pathogenic T(H)17 cells. *Nat Immunol.* 2017;18(1):74–85.
65. Gao F, Du W, Zafar MI, et al. 4-Hydroxyisoleucine ameliorates an insulin resistant-like state in 3T3-L1 adipocytes by regulating TACE/TIMP3 expression. *Drug Des Devel Ther.* 2015;9:5727–5736.
66. Hershko Y, Levytskyi K, Rannon E, et al. Phenotypic and genotypic analysis of antimicrobial resistance in Nocardia species. *J Antimicrob Chemother.* 2023:2306–2314.
67. Tenover FC. Mechanisms of antimicrobial resistance in bacteria. *Am J Med.* 2006;119(6 Suppl 1):S3–S10; discussion S62-S70.
68. Noble WC, Virani Z, Cree RG. Co-transfer of vancomycin and other resistance genes from Enterococcus faecalis NCTC 12201 to Staphylococcus aureus. *FEMS Microbiol Lett.* 1992;72(2):195–198.
69. Severin A, Tabei K, Tenover F, Chung M, Clarke N, Tomasz A. High level oxacillin and vancomycin resistance and altered cell wall composition in Staphylococcus aureus carrying the staphylococcal mecA and the enterococcal vanA gene complex. *J Biol Chem.* 2004;279(5):3398–3407.
70. Perichon B, Courvalin P. Heterologous expression of the enterococcal vanA operon in methicillin-resistant Staphylococcus aureus. *Antimicrob Agents Chemother.* 2004;48(11):4281–4285.

Investigative Ophthalmology & Visual Science